Preparation and Characterization of Aliphatic Polyurethane and Hydroxyapatite Composite Scaffold

Haohuai Liu,[1,2] Li Zhang,[1] Yi Zuo,[1] Li Wang,[1] Di Huang,[1] Juan Shen,[1] Pujiang Shi,[1] Yubao Li[1]

[1]*The Research Center for Nano-Biomaterials, Analytical and Testing Center, Sichuan University, Chengdu 610064, China*
[2]*National Institute of Measurement and Testing Technology, Chengdu 610021, Sichuan, China*

Received 23 September 2008; accepted 6 December 2008
DOI 10.1002/app.29862
Published online 24 February 2009 in Wiley InterScience (www.interscience.wiley.com).

ABSTRACT: Novel porous composite scaffolds for tissue engineering were prepared from aliphatic biodegradable polyurethane (PU) elastomer and hydroxyapatite (HA). It was found that the aliphatic PU was possible to load up to 50 wt % HA. The morphology and properties of the scaffolds were characterized by scanning electron microscope, X-ray diffraction, infrared absorption spectra, mechanical testing, dynamic mechanical analysis, and *in vitro* degradation measurement. The results indicated that the HA/PU scaffolds had an interconnected porous structure with a pore size mainly ranging from 300 to 900 μm, and 50–200 μm micropores existed on the pores' walls. The average pore size of macropores and micropores are 510 and 100 μm, respectively. The compressive strength of the composite scaffolds showed higher enhancement with increasing HA content. In addition, the polymer matrix was completely composed of aliphatic component and exhibited progressive mass loss *in vitro* degradation, and the degradation rate depended on the HA content in PU matrix. The porous HA/PU composite may have a good prospect to be used as scaffold for tissue engineering. © 2009 Wiley Periodicals, Inc. J Appl Polym Sci 112: 2968–2975, 2009

Key words: aliphatic polyurethane; hydroxyapatite; composite scaffold; porous; biodegradable

INTRODUCTION

Currently, there is a great interest on the development of biodegradable polymers suitable for a variety of biomedical applications, such as temporary scaffolds that facilitate tissue regeneration[1–4] or matrices for controlled drug release.[5–9] For a number of implantable devices it would be beneficial to use elastomeric bioresorbable polymers over the rigid ones. After almost half a century of use in the health field, polyurethanes (PUs) remain one of the most popular groups of biomaterials applied for medical devices. Their popularity has been sustained as a direct result of their segmented block copolymeric character, which endows them with a wide range of versatility in terms of tailoring their physical properties, blood and tissue compatibility,[10] and more recently their biodegradation.[1,6]

In addition to the physical properties of PU, a great care has to be taken in the choice of building blocks, because the intended use of the biodegradable polymer is to be inserted in a living organism. The degradation products of PU have to be biocompatible, nontoxic, and metabolized or eliminated by the living organism. Conventional PU polymers are often based on 4,4′-diphenylmethane diisocyanate (MDI) or toluene diisocyanate (TDI), but the aromatic diisocyanate typically used in the hard segment of conventional PU has no good biocompatibility. The degradation products of these aromatic diisocyanates include toxic and carcinogenic compounds such as aromatic diamines, thereby making them undesirable for use *in vivo*.[6] However, PUs prepared from aliphatic polyisocyanates have been reported to degrade into nontoxic decomposition products,[2,4,11] and therefore, aliphatic diisocyanates are preferred over conventional aromatic diisocyanates.

On the other hand, hydroxyapatite (HA) with a structural formula of $Ca_{10}(PO_4)_6(OH)_2$ is the major inorganic component of human bones and teeth. HA has long been used in clinical applications for the filling of bone defects because of its good biocompatibility and bioactivity. It can form bone bonding with living tissue through osteoconductive mechanism.[12–14] Polymers combined with HA are capable of promoting osteoblast adhesion, migration, differentiation, and proliferation.[15–19] In recent years, composite materials composed of bioactive inorganic HA particles and organic polymers have been studied extensively, such as HA/PMMA (polymethyl methacrylate),[20,21] HA/PLA (polylactic acid),[19,22] HA/PE(polyethylene),[16,23] HA/PA(polyamide),[15,17]

Correspondence to: Y. Li (nic7504@scu.edu.cn).
Contract grant sponsor: China-Netherlands Programme Strategic Alliances; contract grant number: 2008DFB50120.
Contract grant sponsor: China 973; contract grant number: 2007CB936102.

HA/PLGA [poly(lactide-*co*-glycolide)],[18,24] HA/PHA (polyhydroxyalkanoates),[25] HA/polycaprolactone (PCL),[26–28] etc.

With the beneficial combination of the reinforcing effect and bioactivity of HA and the adjustable biodegradability of polymer matrices, biodegradable and nontoxic porous HA/PU scaffolds were prepared in this experiment based on 4,4′-dicyclohexylmethane diisocyanate (H_{12}MDI), castor oil (CO), PCL diols (PCL), 1,4-butanediol (BDO), and HA. Among which, stannous octoate, a food stabilizer approved by American FDA, was used as a catalyst. The bulk structures and properties of the scaffolds were characterized by analytical instrument.

EXPERIMENT

Materials and methods

PCL (MW = 1250), CO, and BDO were dehydrated at 100–110°C under vacuum for 2 h, respectively. H_{12}MDI and stannous octoate obtained from Sigma-Aldrich (St. Louis, MO) were used directly. HA, prepared by our group using the method of wet synthesis and hydrothermal treatment,[29] was dried at 100°C for 24 h and then ground and screened through a 75-μm mesh sieve (Kelong Chemicals of Chengdu, Chengdu, China).

The synthesis was carried out in a 250-mL three-necked flask under a dry nitrogen atmosphere using a two-step *in situ* polymerization. The molar ratio of the reaction was 2.25 : 1 : 1 of H_{12}MDI : soft segment (CO+PCL) : chain extender(BDO) and the molar ratio of PCL in soft segment was 50 wt % (PCL : CO = 1 : 1). In the first step of polymerization, HA, PCL, and CO were mixed together, and then, H_{12}MDI and 0.1 wt % stannous octoate were added to the stirring mixture at 80°C under a dry nitrogen atmosphere. In the second step, after stirring for 4 h at 80°C, chain-extender BDO was added to the melting reaction mixture, and the temperature of the reacting mixture was maintained at 65°C. After 3 h, a calculated amount of water was added dropwise to the melting mixture. When the foam was formed, it was annealed in an oven at 120°C for 5 h to complete the reaction, and thus a porous scaffold sample composed of HA and PU were prepared after fully washing by deionized water and dried at 50°C for 24 h. Porous HA/PU scaffold samples with different HA contents were prepared using the same procedure.

Scaffold characterization

SEM observation

A scanning electron microscope (SEM, Hitachi model S-4800, Tokyo, Japan) was employed to observe the porous structure of the scaffolds. The samples were sputtered with a thin gold layer and the test was carried out at 1.0 kV.

The pore size was evaluated from the SEM photographs with image analysis software, Image Pro Plus (Media Cybernetics, USA). Diameters of 100 pores were measured, and the average of pore size was calculated.

XRD analysis

XRD measurements were performed using X-ray diffraction (XRD, X'Per Pro MPD, Philip, The Netherlands) with Cu Kα X-ray source and 3° incident angle and scan range from 10° to 70° (2θ).

FTIR analysis

The Fourier transform infrared (FTIR) analyses of the scaffolds were recorded using a Nicolet 5700 FTIR spectrophotometer in a wavenumber range of 400–4000 cm^{-1}.

Scaffold porosity

Scaffold porosity was determined using a liquid displacement method similar to that reported by Zhangand and Ma[23] and Guan et al.[3] A scaffold sample was immersed in a cylinder containing a certain volume of ethanol (V_1). The sample was kept in ethanol for 5 min to allow the ethanol to penetrate and fill the pores of sample. The total volume of ethanol and the ethanol-impregnated scaffold was recorded as V_2. The ethanol-impregnated scaffold was removed from the cylinder, and the residual ethanol volume was recorded as V_3. The porosity (P) of the scaffold was calculated according to the formula (1), and five samples were evaluated for each scaffold.

$$P = (V_1 - V_3)/(V_2 - V_3) \quad (1)$$

Water vapor permeability

The water vapor permeability (WVP) of the scaffolds was measured according to ASTM method E 96 Desiccant method, i.e., specimens with a thickness of 2–3 mm were placed in an open cup containing silica gel, the edges of the specimens were thoroughly sealed to prevent the passage of water vapor into, out of, or around the specimen edges or any portion thereof. Then, the assembly was placed in a test chamber at 22°C with a constant relative humidity of 60%. Finally, the weight change of permeation cup with the specimen was recorded and the WVP was calculated by the following eq. (2).[30] Results of WVP were expressed as [(g mm)/(m^2 h Pa)]:

$$\mathrm{WVP} = wx/tA\Delta P \quad (2)$$

where x is the average thickness of the specimens, w is the weight change of permeation cup with the specimen (g), t is the assembly time in the test chamber (h), A is the area of permeation (m^2), and ΔP is the difference of partial vapor pressure of atmosphere with silica gel and pure water. An average of three parallel samples was used for each WVP measurement.

Mechanical properties

For mechanical testing, samples were cut into cylinders with a diameter of 10 mm and length of 20 mm. The test was run at a crosshead speed of 1 mm/min in the direction perpendicular to the diameter. The compressive strength at 60% of deformation and the Young's modulus were calculated as the slope of the initial linear portion of the stress–strain curve. All the given values were the means of five measurements.

Dynamic mechanical analysis

Dynamic mechanical analysis (DMA) was studied on TA Q800 (TA Instrument, USA) analyzer. The samples were trimmed to the dimensions of 35 mm in length, 12 mm in width, and 5 mm in thickness. The properties were measured at the temperature range from −100 to 100°C at a heating rate of 3°C/min. The tests were carried out at a frequency of 1 Hz.

Degradation *in vitro*

To measure the hydrolytic degradation of the scaffold, dry scaffolds ($10 \times 10 \times 10$ mm^3) were weighed and placed into glass ampoules filled with phosphate buffer solution ($pH = 7.4 \pm 0.2$). The phosphate buffer solution was replaced every 2 weeks. The ampoules were kept at 37°C ± 0.1°C in an incubator for 1, 2, 4, 6, 8, 10, and 12 week(s). Samples were removed at the time point from the phosphate buffer solution, rinsed three times with distilled water, and dried to a constant weight at 60°C under vacuum to determine the weight loss ratio. The weight loss ratio was calculated as follows:

$$\text{Weight loss ratio} = (w_1 - w_2)/w_1 \times 100\% \quad (3)$$

where w_1 and w_2 are the weights of samples before and after degradation *in vitro*, respectively. Five samples were tested for each time interval, and the mean value was taken to calculate the weight loss.

RESULTS

Formation mechanism of the porous structure

The porous structure of HA/PU composite are formed directly from the two-step reaction. In the first step, the polyol reacts with excess diisocyanate to obtain a macrodiisocyanate with the urethane linkages. In the second step, chain extender and water are added to the macrodiisocyanate. The reaction of the isocyanate groups with water results in the formation of transient carbamic acid, an amine, and carbon dioxide. The formation of carbon dioxide makes the polymer produce a porous structure. It should be stressed here that CO, which has been proved to possess good foamability, is not only a polyol candidate in the successful formation of PU but also helps to form the porous structure.

Morphology of the scaffolds

The three-dimensional gross morphology and SEM photographs of the porous structure are shown in Figure 1. Figure 1(a,b) shows the sample with 30 wt % HA, Figure 1(c,d) shows the sample with 40 wt % HA, Figure 1(e,f) shows the sample with 50 wt % HA, and Figure 1(g,h) shows the sample with 60 wt % HA. The results indicate that the porous scaffolds containing a HA content from 30 to 50 wt % exhibit highly porous structure with a porosity more than 80%. The pore size of these scaffolds mainly ranges from 300 to 900 μm, and many micropores with a size of 50–200 μm distribute on the walls of the macropores. The average pore size of macropores and micropores are 510 and 100 μm, respectively. It is just the micropores that make the composite show an interconnected porous structure, which is beneficial for improving the adhesion of cells, the invasion of blood vessels and tissues, as well as the nutrient cycling. It has been reported that bone ingrowth requires the scaffold to have open and interconnected pores with a porosity more than 70% and a pore size larger than 150 μm,[14] which is also favorable for the proper circulation of nutrients.

WVP of the scaffolds is listed in Table I. It shows that the scaffolds with HA content from 30 to 50 wt % have a higher water permeability from 3.28×10^{-2} to 3.44×10^{-2} (g mm)/(m^2 h Pa) than the scaffold with 60 wt % HA. The scaffold with 60 wt % HA shows a low WVP [0.82×10^{-2} (g mm)/(m^2 h Pa)]. It indicates that the scaffolds with more open and interconnected pores have higher WVP.

The scaffold with 60 wt % HA shows much lower porosity (43.2 ± 2.5%) and smaller pore size, and the water permeability is also very low, which indicates a high number of closed pores present in the scaffold. This should be attributed to the excessive HA content in composite, which makes the melting PU prepolymer too viscous. The higher viscosity does not allow the homogeneous mixing of water into prepolymer. It is important that the PU prepolymer is sufficiently viscous before the initiation of the reaction with water so that all monomers have been reacted thoroughly and the rising foam does not collapse on itself before curing. However, if it is too viscous, water cannot be thoroughly and homogeneously mixed into the

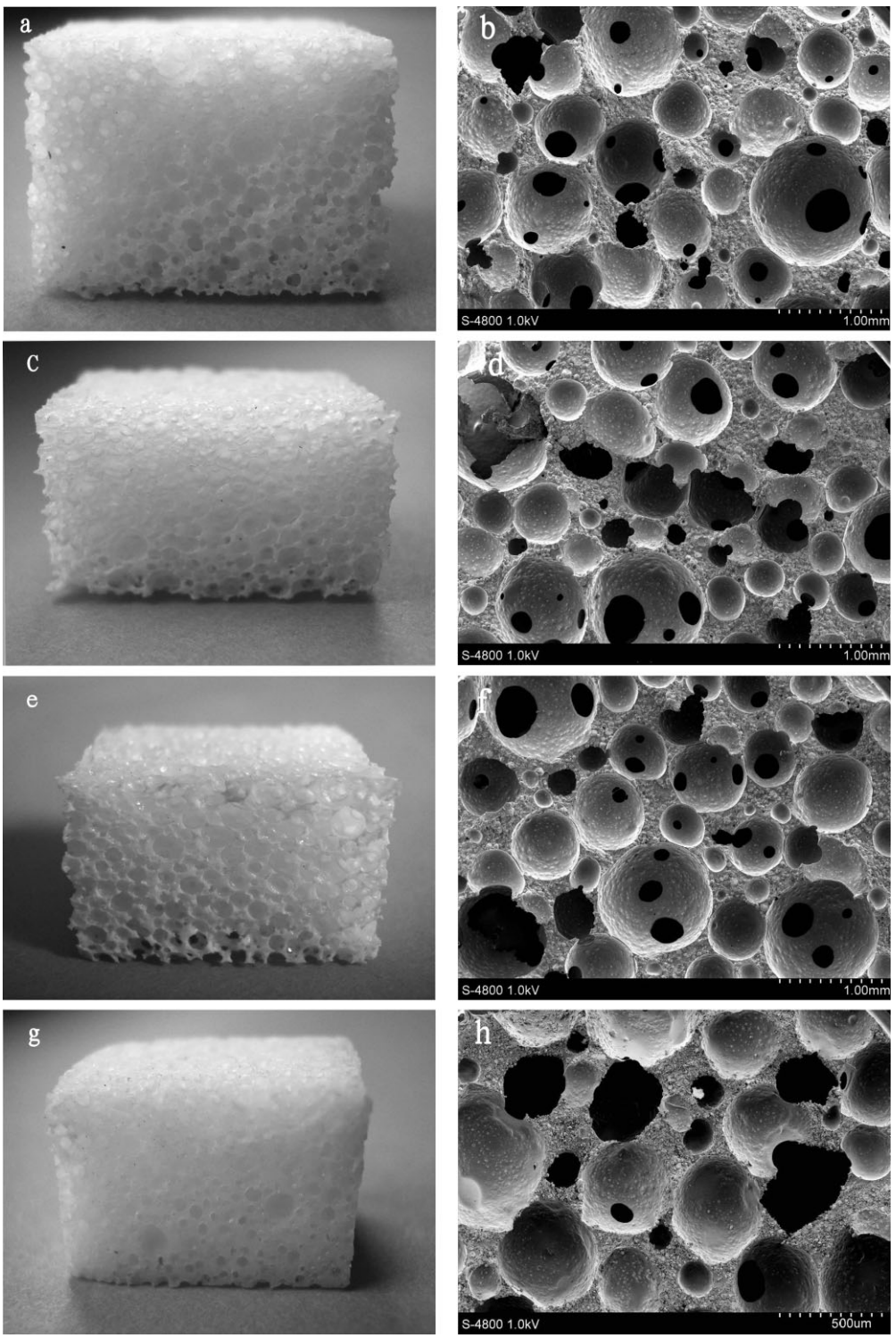

Figure 1 Photographs of the porous HA/PU composite scaffolds: (a and b) 30 wt % HA; (c and d) 40 wt % HA; (e and f) 50 wt % HA; and (g and h) 60 wt % HA (a, c, e, and g from photomacrograph and b, d, f, and h from SEM).

prepolymer when initiating the foaming reaction.[31] If the scaffold with higher HA content (such as 60 wt %) has to be selected for tissue engineering, other foaming agents or other oligomer (polyester or polyether) should be used to raise its porosity and enlarge its pore size.

Compressive strength

The stress–strain behaviors of HA/PU scaffolds with HA content from 30 to 50 wt % are shown in Figure 2. Because the porosity of the scaffold with 60 wt % HA does not meet the requirement of more than 70%, its compressive strength and modulus are not tested.

TABLE I
Characteristics of HA/PU Composite Scaffolds

HA content (wt %)	Porosity (%)	Average pore size (μm)	WVP (10^{-2}) [(g mm)/(m^2 h Pa)]	Compressive strength (kPa)	Modulus (kPa)
30	82.8 ± 2.6	517 ± 40	3.44 ± 0.2	227 ± 28	607 ± 27
40	83.7 ± 2.8	503 ± 50	3.28 ± 0.3	388 ± 35	1001 ± 32
50	82.4 ± 2.3	510 ± 45	3.40 ± 0.2	548 ± 37	1608 ± 40
60[a]	43.2 ± 2.5	186 ± 21	0.82 ± 0.09	–	–

[a] The porosity of the scaffold with 60 wt % HA does not meet the requirement of more than 70%, and therefore its compressive strength and modulus are not tested.

The mechanical parameters corresponding to Figure 2 are listed in Table I. It is found that HA content has a remarkable effect on the strength of the composite scaffolds. When the HA content is from 30 to 50 wt % in the composites, the porous scaffolds have a compressive strength from 227 to 548 kPa and a modulus from 607 to 1608 kPa. The result indicates that the compressive strength and modulus increase dramatically with the increase of HA content.

It can be seen from Table I that the 50 wt % scaffold has the highest compressive strength and modulus comparing with those of 30 and 40 wt % scaffolds. The result illustrates that 50 wt % addition of HA content is appropriate in the PU matrix when comprehensively considering the requirement of bioactivity, pore size, porosity, and mechanical strength for tissue engineering scaffold.

XRD patterns

Figure 3 shows the XRD patterns of HA, PU, and HA/PU composite, in which curve a indicates pure HA crystals, curve b is for HA/PU composite, and curve c is for pure PU. It can be seen from Figure 3(a) that HA crystals are in a state of weak crystallized apatite structure, and the major characteristic peaks of HA at $2\theta = 25.9°$, 31.9°, 33°, 34°, and 40°, which are in accord with those of bone apatite.[32] The pure PU pattern in Figure 3(c) is amorphous and exhibits a broad diffraction envelop from 15° to 25° in 2θ. In Figure 3(b), the intensities of HA peaks become weaker in the presence of PU, and by calculation from XRD patterns, the crystallinity of HA in composite decreases from 52.1 to 43.6% when compared with that of pure HA. However, no peak shift of HA in the composite can be found, which means after being compounded with PU, the nature of HA does not change. In addition, the broad diffraction peak of PU at 15°–25° also presents a decrease, and this may attributed to the destruction of HA incorporation on the organization of PU chains, decreasing the orderliness of structure array in PU.

FTIR spectra

The HA spectrum in Figure 4 shows the presence of —OH^- (3571 cm^{-1}), H_2O (3400 cm^{-1}, 1638 cm^{-1}), —PO_4^{3-} (1093 cm^{-1}, 1035 cm^{-1}), and —CO_3^{2-} (1384 cm^{-1}) in the HA crystals. These characteristic peaks also exist in the infrared (IR) spectrum of bone apatite.[33,34] This further proves the similarity of the HA

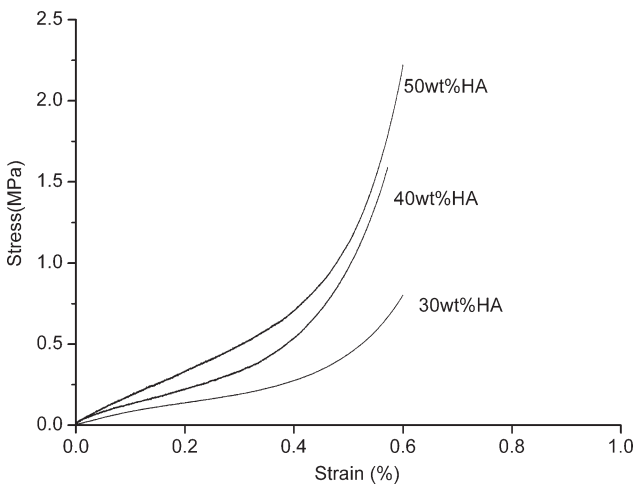

Figure 2 Compressive stress–strain curves for HA/PU composite scaffolds.

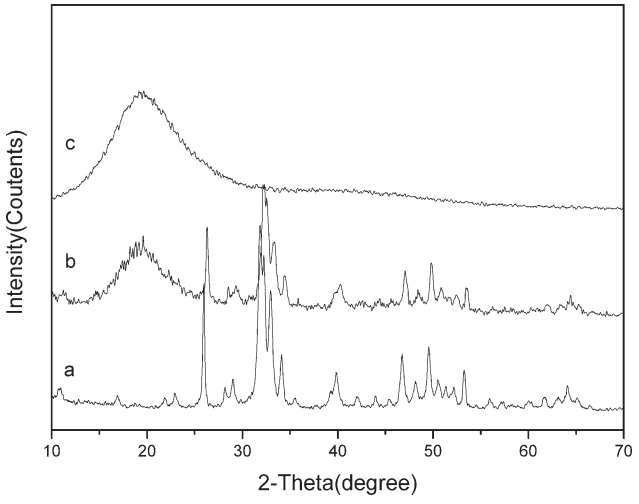

Figure 3 XRD patterns of HA (a), HA/PU composite (b), and PU (c).

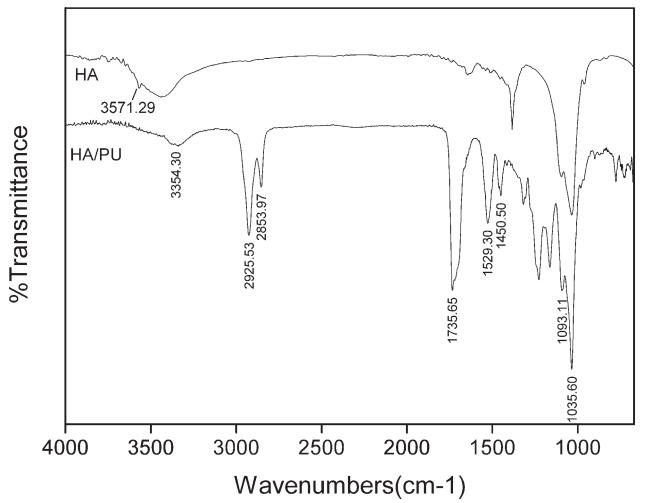

Figure 4 IR spectra of HA and HA/PU composites.

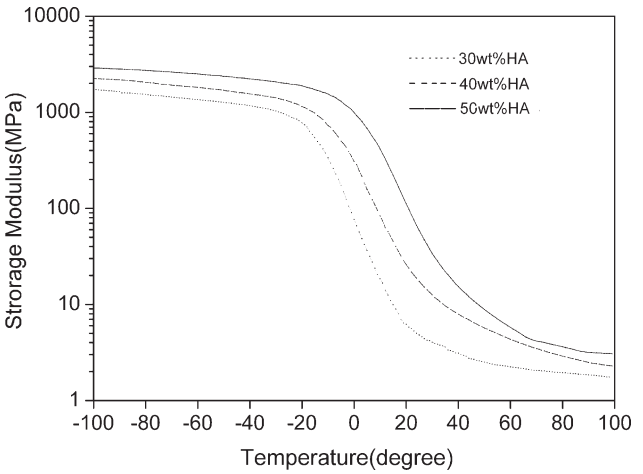

Figure 5 Storage modulus (E') versus temperature for PU/HA scaffolds.

crystals to bone apatite. The FTIR spectrum of HA/PU in Figure 4 indicates that the characteristic frequencies of urethane linkage at around 1735 cm^{-1} is for >C=O stretching, whereas the >C=O stretching vibration of ester is overlapped in the urethane linkage, resulting in a strong peak at 1735 cm^{-1}. N—H stretching vibration of the urethane linkage is observed near 3354 cm^{-1}, which indicates that most of the amide groups in PU are involved in hydrogen bonds, because free N—H stretching peak of PU is usually manifested by the band at 3445–3450 cm^{-1}.[35,36] In the spectrum, the sharp bands at 2925 and 2853 cm^{-1} are attributed to the asymmetric and symmetric stretching vibrations of the methylene group (—CH_2), whereas other mode of —CH_2 vibration is manifested by the band at 1450 cm^{-1}. The band at 1529 cm^{-1} is assigned to amide II aliphatic R—NH—COO— groups. Peaks at 1093 cm^{-1} and 1035 cm^{-1} belong to the phosphate radical group (—PO_4^{3-}) of HA. The absence of —NCO absorption band at 2250–2270 cm^{-1} and —OH peak at 3571 cm^{-1} in HA/PU spectrum in Figure 4 illustrate that the isocyanate groups and hydroxyl groups had reacted completely.

Dynamic mechanical analysis

The storage modulus (E') as a function of temperature for PUs with different HA content is shown in Figure 5. It is clear that the storage modulus of all three samples decreases with the increase of temperature, and with increasing HA content, the storage modulus of HA/PU scaffolds can significantly be increased over the whole temperature range. This result indicates that the incorporation of HA into PU has a good reinforcing effect, which may originate from the stiff HA particles and the interaction between the filler and matrix.

The variation of dissipation factor (tan δ) with temperature for the scaffolds is given in Figure 6. The top peak in each curve corresponds to the glass transition temperature (T_g) of the composites. It can be seen that the T_g value rises with the increase of HA content in composites, which may ascribe to the restriction of PU chain mobility by the presence of HA. The increase of T_g temperature indicates a better interaction or reinforcement between the filler and matrix.

Degradation *in vitro*

The curves of the weight loss as a function of immersion time are shown in Figure 7. It can be seen that all the three scaffolds exhibit a progressive mass loss over the 12-week period. The ratio of weight loss ranges from 10.63 to 15.87% at 12 weeks depending on the HA content. The scaffold with low HA content has higher degradation rate than the scaffold with

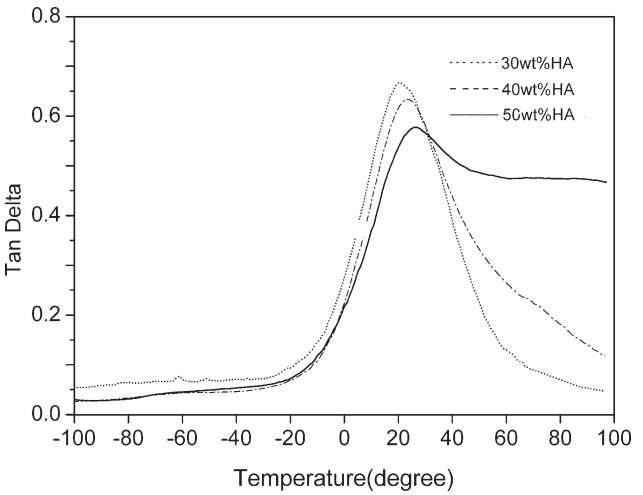

Figure 6 Variation of tan δ as a function of temperature for PU/HA scaffolds.

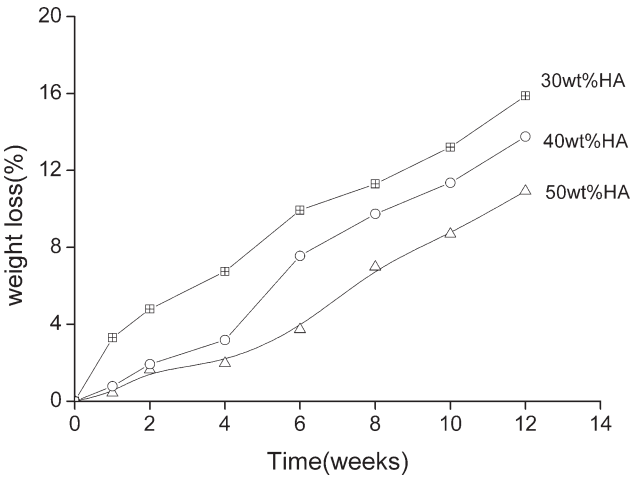

Figure 7 The weight loss of HA/PU composite scaffolds for different immersion time.

high HA content. This indicates that the weight loss is mainly caused by the degradation of PU matrix. It is worth noting that this preliminary study has examined the degradation in the absence of plasma enzymes and cells. Degradation in a cell culture or *in vivo* environment can be expected to be faster.[3]

DISCUSSION

There is a continuing interest in designing new polymeric materials in a form of porous scaffolds, which can be used as tissue substitutes to repair or, preferably, regenerate damaged tissues. Commercially available PUs exhibit good mechanical properties, but they often have a disadvantage of containing aromatic MDI. PUs based on MDI are known to release carcinogenic and mutagenic products when being degraded.[6] In this study, it is expected to prepare novel aliphatic PU composite for biomedical applications. The polymer matrix completely consists of aliphatic components and only releases nontoxic degradation products. Herein, H_{12}MDI is selected to replace MDI, PCL diols and CO are chosen to react with H_{12}MDI to form a new kind of polyesterurethane. Previously, PCL has been investigated as a matrix for a totally bioresorbable composite for craniofacial reconstruction[22] and known to be biocompatible and slowly degradable hydrolytically and enzymatically.[37] However, CO has been used as a promising raw material for the preparation of biodegradable PUs because of its low cost, nontoxicity, hydrolyzation, and its availability as a renewable agricultural resource.[38]

In addition, HA has a composition and structure very close to bone apatite and therefore has been considered to be the ideal material to build bone tissue engineering scaffold. To mimic the composition of bone apatite and to enhance the bioactivity and mechanical strength of the scaffold, we chose HA and elastomeric biodegradable PU to prepare porous composite scaffolds. Using elastomeric cancellous bone graft to fill bone defects may ensure an intimate contact with the native bone ends, avoid shear forces at the bone–implant interface, a phenomenon that is unavoidable in the case of rigid materials. The addition of HA may improve cell proliferation on and in the scaffold and, in consequence, promote healing of bone defects.

Scaffolds for tissue repair and regeneration should preferably be porous to allow the transportation of nutrients and the ingrowth of cells, capillaries and tissues, and also be bioresorbable and/or biodegradable to allow the replacement by newly formed tissues. Furthermore, they should possess three-dimensionally porous structure with a porosity more than 70% and pore size ranging from 50 to 900 μm.[39–41] In this study, HA/PU composite scaffolds have good interconnected porous structure with typical pore size ranging from 300 to 900 μm, and there are micropores on the walls of macropores in the range 50–200 μm. The average pore size of macropores and micropores are 510 and 100 μm, respectively. Also, the porosity of the scaffolds is more than 80%, making the surface area of the scaffold increase, which is very important for promoting the adhesion and growth of the planting cells and accelerating the tissue regeneration.

It is well known that bone scaffold should not only have high porosity but also proper mechanical property and degradation, which can match with the growth of new bone tissues. In this work, the compressive strength and modulus of scaffolds increase dramatically with the HA content. Especially, the scaffold with 50 wt % HA has a compressive strength of 548 kPa and a modulus of 1608 kPa. This is sufficiently high for the regeneration of cartilage tissues[42] and for the filling of large bone defects. The scaffold exhibits good mechanical property because of the homogeneous dispersion of HA particles in PU matrix. Considering the reinforcing effect of the HA filler and the open porous structure of the composite, the optimal addition of HA in PU can be 50 wt %.

The hydrolytic degradation of PUs in the aqueous media often proceeds mainly via the scission of the ester, urethane, or urea linkage in the main chains. In polyesterurethane, water reacts with the carboxylic ester bonds of PCL and CO, breaking the polymer chain into two shorter ones. One ending is a hydroxyl group while the other is a carboxyl group as shown in expression (4). The acidic carboxyl group accelerates further hydrolysis of the polyester segments and the degradation becomes autocatalytic.[2,43]

$$\mathrm{RCOOR'} + \mathrm{H_2O} \rightarrow \mathrm{RCOOH} + \mathrm{R'OH} \qquad (4)$$

The urethane or urea linkage can also be hydrolyzed, and the hydrolysis also produces two shorter chains, one ending is the hydroxyl group and the

other is the amino group shown in expression (5). These groups do not appear to autocatalyze the hydrolysis of PUs.[4]

$$\mathrm{RNHCOOR' + H_2O \rightarrow RNHCOOH + R'OH} \quad (5)$$

However, the hydrolysis of the urethane or urea linkage is more difficult than carboxylic ester linkage, and therefore, the cleavage of the carboxylic ester group in this study is the predominant process.

The degradation of the scaffolds *in vitro* is manifested by mass loss (Fig. 7). The scaffold containing 50 wt % HA shows 10.63% weight loss when compared with the initial mass after 12-week immersion, whereas the scaffolds containing 30 and 40 wt % HA exhibit 15.87% and 13.76% weight loss, respectively. These results demonstrate that the scaffold with low HA content will have higher degradation rate than that with high HA content. This is attributed to that the increase in HA content in the composite decreases the availability of more PU polymer to hydrolysis.

CONCLUSION

The HA/PU scaffolds developed in this study were designed for tissue engineering application. HA crystals were added into PU matrix to promote the osteoconductive properties of the scaffold. The results indicated that the aliphatic PU could load HA up to 50 wt %, and the composite showed good mechanical properties due to the reinforcement of HA. The composite scaffolds exhibited highly porous structure with a porosity of more than 80%. The macropore size of the porous scaffold ranged from 300 to 900 μm and many micropores with a size of 50–200 μm present on the walls of macropores. The average pore size of macropores and micropores are 510 and 100 μm, respectively. In addition, the scaffold exhibited progressive degradation *in vitro* taken by the mass loss and the degradation rate depended on the HA content in PU matrix. Certainly, many questions such as cell phenotype retention and *in vivo* behavior of the construct remain to be solved and will be addressed in new studies. The primary investigation of the aliphatic HA/PU scaffold shows a potential for cancellous bone substitutes. The elastomeric composite scaffold may enhance cell proliferation into the scaffold and, in consequence, promote healing of bone defects.

References

1. Guelcher, S. A. Tissue Eng Part B Rev 2008, 14, 3.
2. Gornaand, K.; Gogolewski, S. J Biomed Mater Res A 2003, 67, 813.
3. Guan, J. J.; Fujimoto, K. L.; Sacksand, M. S.; Wagner, W. R. Biomaterials 2005, 26, 3961.
4. Kavlock, K. D.; Pechar, T. W.; Hollinger, J. O.; Guelcherand, S. A.; Goldstein, A. S. Acta Biomater 2007, 3, 475.
5. Chasin, M.; Langer, R. Biodegradable Polymers as Drug Delivery Systems; Marcel Dekker: New York, 1990.
6. Santerre, J. P.; Woodhouse, K.; Larocheand, G.; Labow, R. S. Biomaterials 2005, 26, 7457.
7. Zhang, C.; Zhao, K.; Hu, T.; Cui, X.; Brownand, N.; Boland, T. J Controlled Release 2008, 131, 128.
8. Sivak, W. N.; Pollack, I. F.; Petoud, S.; Zamboni, W. C.; Zhangand, J.; Beckman, E. J. Acta Biomater 2008, 4, 852.
9. Piozzi, A.; Francolini, I.; Occhiaperti, L.; Vendittiand, M.; Marconi, W. Int J Pharm 2004, 280, 173.
10. Lelah, M.D.; Cooper, S. Polyurethanes in Medicine; CRC Press: Boca Raton, FL, 1986.
11. Guan, J. J.; Sacks, M. S.; Beckmanand, E. J.; Wagner, W. R. J Biomed Mater Res 2002, 61, 493.
12. Hench, L. L.; Wilson, J. Science 1984, 226, 630.
13. Shackelford, J. F. Bioceramics 1999, 293, 99.
14. Cerroni, L.; Filocamo, R.; Fabbri, M.; Piconi, C.; Caropresoand, S.; Condò, S. G. Biomol Eng 2002, 19, 119.
15. Jieand, W.; Li, Y. Eur Polym J 2004, 40, 509.
16. Wang, M.; Deband, S.; Bonfield, W. Mater Lett 2000, 44, 119.
17. Wang, H. N.; Li, Y. B.; Zuo, Y.; Li, J. H.; Maand, S. S.; Cheng, L. Biomaterials 2007, 28, 3338.
18. Lee, J. B.; Lee, S. H.; Yu, S. M.; Park, J.-C.; Choiand, J. B.; Kim, J. K. Surf Coat Technol 2008, 202, 5757.
19. Nejati, E.; Mirzadehand, H.; Zandi, M. Compos Part A Appl Sci Manuf 2008, 39, 1589.
20. Monvisade, P.; Siriphannon, P.; Jermsungnernand, R.; Rattanabodee, S. J Mater Sci Mater Med 2007, 18, 1955.
21. Shyang, C. W.; Khim, L. Y.; Ariffin, A.; Arifinand, Z.; Ishak, M. J Reinf Plast Compos 2008, 27, 945.
22. Corden, T. J.; Jones, I. A.; Rudd, C. D.; Christian, P.; Downesand, S.; McDougall, K. E. Biomaterials 2000, 21, 713.
23. Zhangand, R. Y.; Ma, P. X. J Biomed Mater Res 1999, 44, 446.
24. Nieand, H.; Wang, C.-H. J Controlled Release 2007, 120, 111.
25. Shishatskaya, E. I.; Khlusovand, I. A.; Volova, T. G. J Biomater Sci Polym Ed 2006, 17, 481.
26. Zhao, J.; Guo, L. Y.; Yangand, X. B.; Weng, J. Appl Surf Sci, to appear.
27. Kim, H.-W.; Knowlesand, J. C.; Kim, H.-E. Biomaterials 2004, 25, 1279.
28. Shor, L.; Güçeri, S.; Wen, X.; Gandhiand, M.; Sun, W. Biomaterials 2007, 28, 5291.
29. de Wiln, J.; Li, Y.; Klein, C. P. A. T.; Meer, S. V. D.; de Groot, K. J Mater Sci: Mater Med 1994, 5, 252.
30. Sobral, P. J. A.; Menegalli, F. C.; Hubingerand, M. D.; Roques, M. A. Food Hydrocolloids 2001, 15, 423.
31. Sivak, W. N.; Pollack, I. F.; Petoud, S.; Zamboni, W. C.; Zhangand, J.; Beckman, E. J. Acta Biomater 2008, 4, 1263.
32. Montel, G.; Bonel, G.; Heugheubaert, M.; Trombe, J. C. J Cryst Growth 1981, 53, 74.
33. Pascalis, E. P.; Betts, F.; DiCarlo, E.; Mendelsohn, R.; Boskey, A. L. Calcif Tissue Int 1997, 61, 480.
34. Rey, C.; Collins, B.; Goehl, T.; Dickson, I. R.; Glimcher, M. J. Calcif Tissue Int 1989, 45, 157.
35. Yilgor, E.; Yilgorand, I.; Yurtsever, E. Polymer 2002, 43, 6551.
36. Wilhelmand, C.; Gardette, J. L. Polymer 1997, 38, 4019.
37. Pena, J.; Corrales, T.; Izquierdo-Barba, I.; Doadrioand, A. L.; Vallet-Regi, M. Polym Degrad Stab 2006, 91, 1424.
38. Yeganehand, H.; Hojati-Talemi, P. Polym Degrad Stab 2007, 92, 480.
39. Salgado, A. J.; Coutinhoand, O. P.; Reis, R. L. Macromol Biosci 2004, 4, 743.
40. Hutmacher, D. W. Biomaterials 2000, 21, 2529.
41. Ma, P. X. Mater Today 2004, 7, 30.
42. Spaans, C. J.; Belgraver, V. W.; Rienstra, O.; de Groot, J. H.; Vethand, R. P. H.; Pennings, A. J. Biomaterials 2000, 21, 2453.
43. Gogolewski, S. Trends Polym Sci 1991, 1, 47.